



Si-TPC with GEMs

A. Bamberger*, H. Blank†, C. Brezina†, K. Desch†, M. Killenberg†,
T. Krautscheid†, W. Ockenfels†, U. Renz*, M. Schumacher*, M. Titov*, M. Ummenhofer†,
N. Vlasov*, P. Wienemann†, S. Zimmermann†, A. Zwerger*

18.12.2008
(Update 21.01.2009)

Abstract

This contribution reports on measurements with a GEM based TPC using the TimePix CMOS ASIC as a charge collecting readout anode. Tests on a small prototype with a 6 mm drift space were performed in a 5 GeV electron beam at DESY. The point resolution for short drift distances is better than 20 μm . A time resolution as good as 8 ns at 100 MHz clock frequency is achieved. Furthermore, experimental studies with an enlarged pixel size are addressed.

Currently an UV/laser test bench is under development. The UV-laser will release single or a few photo electrons from the drift cathode, which are correlated in space and time. This correlation allows detailed studies of detection efficiencies and gas amplification processes in Micro-Pattern-Gas-Detectors.

For the EUDET test beam at DESY a software is developed to integrate the pixel-readout based data acquisition there.

*University of Freiburg, Freiburg, Germany

†University of Bonn, Bonn, Germany

1 Introduction

The development of Micro-Pattern-Gas-Detectors (MPGDs) expands the field of application for detectors based on gas multiplication. The concept of the International Large Detector (ILD) is an excellent candidate for investigating e^+e^- -events at the International Linear Collider (ILC). A Time Projection Chamber (TPC) is foreseen as the central tracking system. The readout concept for this TPC envisages the use of GEMs due to their high rate properties and low ion backdrift. In the module, developed for the Eudet Large Prototype, the pad readout, with a typical pad size in the order of a few mm, will be replaced by a highly integrated device, the TimePix CMOS pixel ASIC. The advantage of this concept is the small pixel size of the TimePix, with $55\ \mu\text{m} \times 55\ \mu\text{m}$ matching the typical granularity of the GEMs. Each pixel has amplifying, shaping and discriminating front-end electronics, which measures either time of arrival or charge amplitude. Tests with a prototype triple GEM/TimePix setup developed at the University of Freiburg are performed in a 5 GeV electron beam at DESY. A supplementary Si-strip-telescope records the electron track position. Two GEMs with different hole- and pitch-geometries are tested. Furthermore, experimental studies with an enlarged pixel size are ongoing. The achieved spatial precision might not be needed in all applications. For example with drift distances above several centimeters the spatial resolution starts to be dominated by transverse diffusion. This is of special importance, because for such a high pixelation, threshold effects become important, since the charge per pixel (pad) is decreasing. For more detailed studies of detection efficiencies for single electrons and of the gas amplification processes in Micro-Pattern-Gas-Detectors a laser test bench is currently setup in Freiburg. An UV-Laser will release single or few electrons from the drift cathode, which are then correlated in space and time. This correlation is crucial to perform the planned studies.

2 Description of the Detector

2.1 GEMs and TimePix

2.1.1 GEMs

A GEM is a thin metal-coated polymer foil with a high density of chemically etched holes arranged in a regular pattern. Two different pitch-geometries are investigated:

- A standard GEM consists of a $50\ \mu\text{m}$ Kapton® layer coated on both sides with $5\ \mu\text{m}$ of Cu, which act as electrodes. The holes with an outer diameter $70\ \mu\text{m}$ have a pitch of $140\ \mu\text{m}$. The active surface is $100\ \text{mm} \times 100\ \text{mm}$. In Fig. 1a a scanning tunneling microscope image of standard GEM is shown.
- A small pitched GEM, like a standard GEM, has the same thicknesses for the Kapton® and copper layers. However the holes have an outer diameter of $30\ \mu\text{m}$ and a pitch of $50\ \mu\text{m}$ and the active surface is $28\ \text{mm} \times 24\ \text{mm}$.

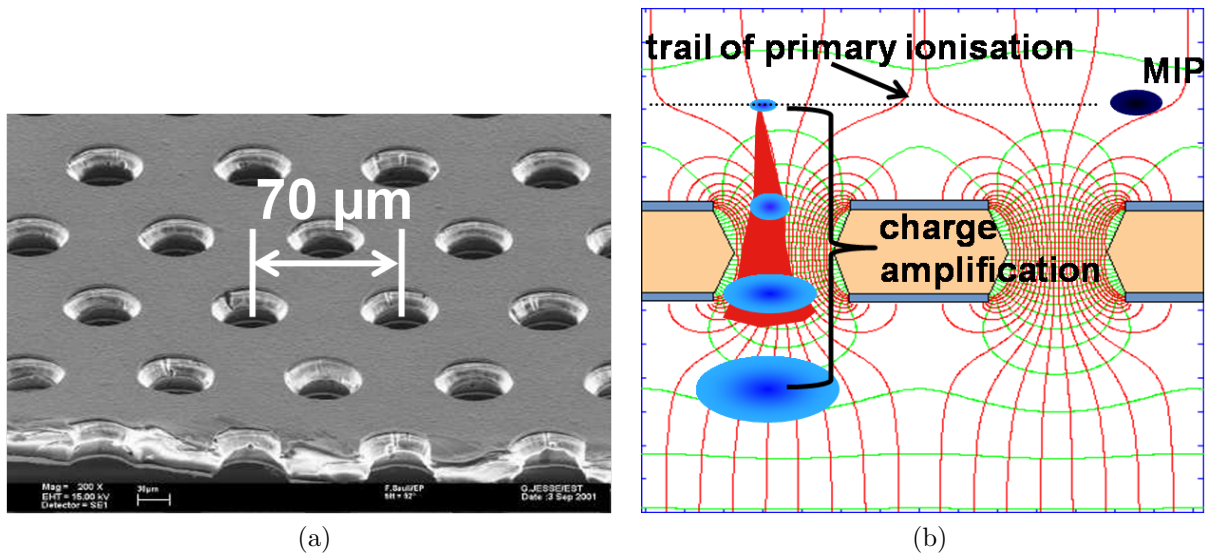


Figure 1: a) Scanning tunneling microscope image of a standard GEM.
 b) Garfield simulation of electrostatic potential (green) and field (red) for two GEM holes.

Fig. 1b shows the electrostatic potential (green) and field (red) for two GEM holes. Above the GEM a Minimum Ionizing Particle (MIP) is represented by a black dot crossing from the left to the right, leaving a trail of primary ionization.

2.1.2 TimePix

The TimePix CMOS readout pixel chip [1] is used as highly segmented charge collecting anode. Fig. 2a shows a TimePix chip installed in the setup. On the chip 65536 pixels are arranged in a square matrix of 256 × 256 lines and columns. As the size of each pixel cell is 55 μm × 55 μm the total active surface is 14 mm × 14 mm. Every pixel is equipped with an amplifying, shaping and discriminating front-end electronic and a linear feedback shift register (LFSR). A reference clock is distributed throughout the entire chip and increments the LFSR depending on the chosen mode of operation. The maximum number of counts is 11810, which is overflow controlled. For each pixel one of the four modes can be set individually:

TOT: In the “Time-Over-Threshold” mode the clock cycles are counted as long as the signal is above an adjustable threshold.

TIME: In TIME-mode the clock cycles are counted from the point the signal crosses the adjusted threshold until a common stop by a gate signal called “shutter”.

MediPix: In the MediPix-mode the number of hits crossing an adjustable threshold are recorded.

OneHit: The first signal crossing the adjusted threshold sets the counter to one. Any further hits will be ignored.

To record simultaneously TIME and TOT information the TimePix is operated in a special mode: in a checkerboard-like fashion consecutive pixels are set to TOT and TIME. Consequently 1/2 of the pixels record TIME, while the other 1/2 record TOT. An illustration of this mixed mode (MM) is given in Fig. 2b.

2.2 Test Beam Setup

The TimePix is positioned at the edge of a triple GEM stack as shown in Fig. 3. For monitoring purposes 24 anode pads of $20\text{ mm} \times 20\text{ mm}$ size cover the remaining active surface of standard GEMs. The GEM stack is operated at a nominal gain of $\approx 10^5$ with an Ar/CO₂ 70/30 gas mixture. The gas tight box contains the GEMs, a resistor chain for distributing the voltages to the stack and the TimePix.

The 5 GeV electron beam transverses a volume with 6 mm drift distance from the right hand side. There are three scintillators installed in the beam: two crossed scintillators upstream and one scintillator downstream. Each of the scintillators is $10\text{ mm} \times 15\text{ mm}$ large. The scintillators accept a beam of $\lesssim 10\text{ mm} \times 10\text{ mm}$ cross section. As displayed in Fig. 3 the setup is positioned in between the two sensor layers of a Si-stripe-telescope [2]. The telescope has a $50\text{ }\mu\text{m}$ readout pitch and is used for external track determination. A MUROS2 [3] interface board is used to readout the TimePix. The coincidence of all three finger counters triggers a gate signal of $100\text{ }\mu\text{s}$ length. The gate signal is brought

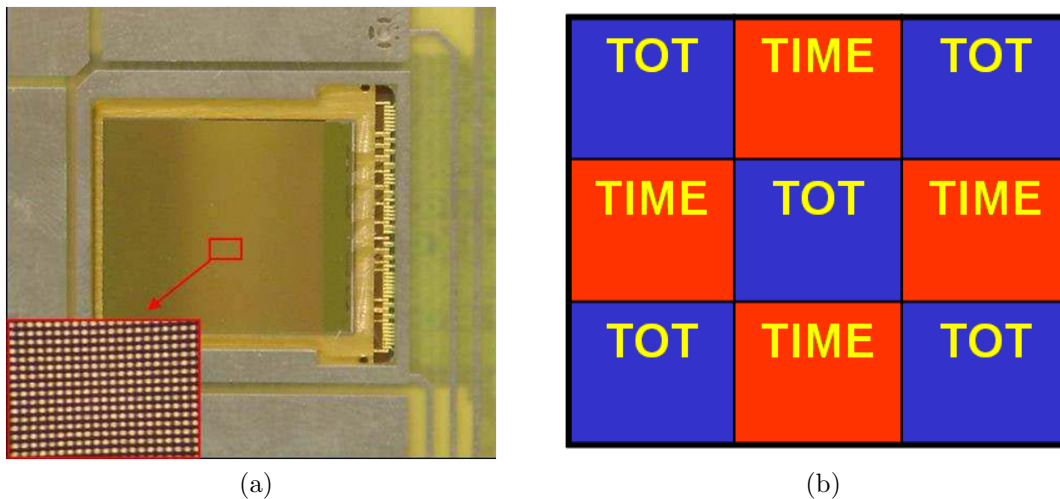


Figure 2: a) Image of a TimePix chip installed in the setup. The inset shows a magnified view of the chip, where single pixels are visible.

b) Pixel for a chip operated in mixed mode "MM" where consecutive pixels are set either to TOT or TIME mode resulting in a checkerboard like pattern.

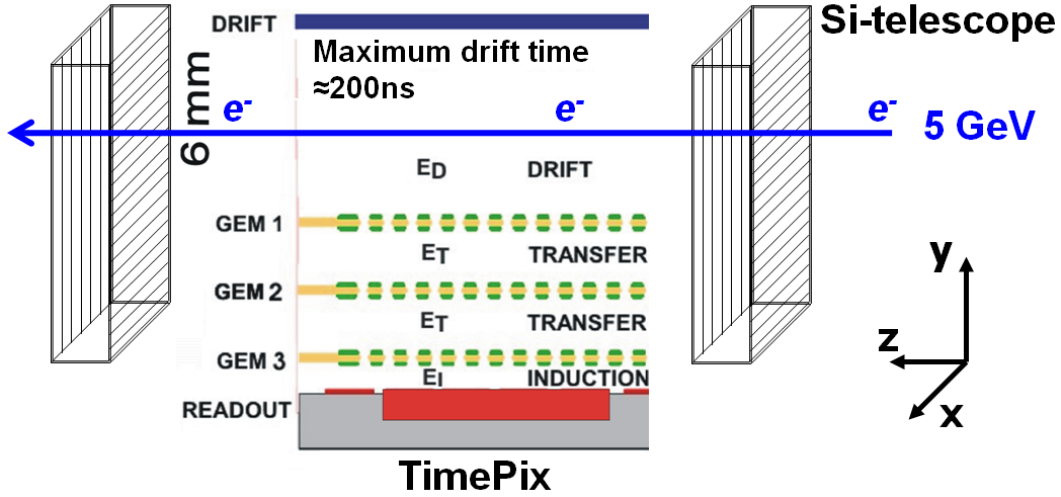


Figure 3: Shown is a vertical cut of the triple GEM stack with the TimePix chip and the two Si-stripe telescope layers used for an external determination of tracks.

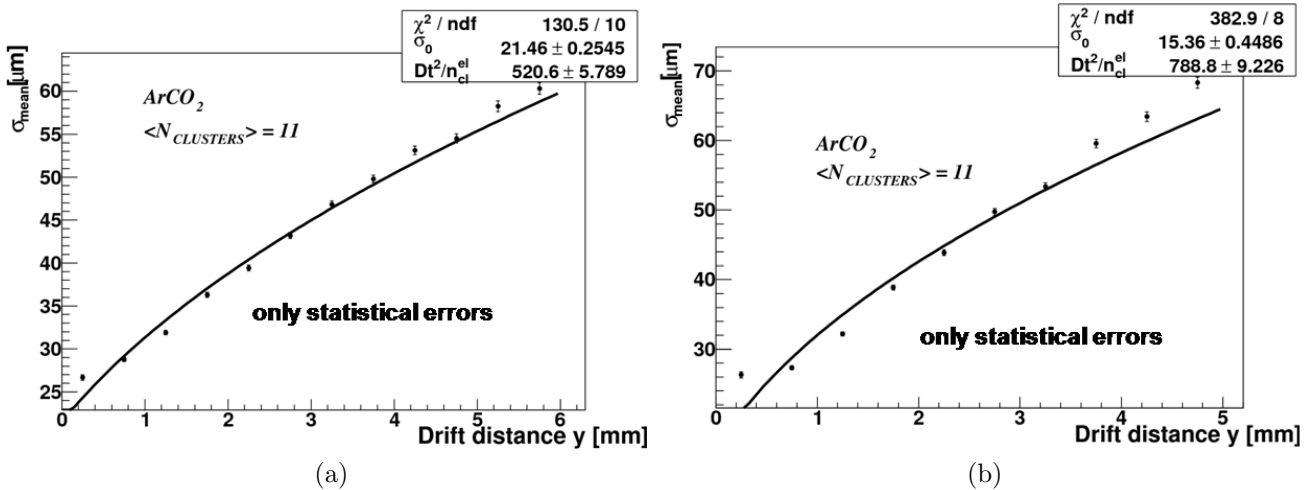


Figure 4: a) Resolution $\sigma_{mean}(y)$ as function of drift distance y for standard GEMs.
 b) Resolution $\sigma_{mean}(y)$ as function of drift distance y for small pitched GEMs.

to the chip via the external “shutter” option of the MUROS2. Only during this time the chip is sensitive for events.

2.3 Spatial Resolution

The spatial resolution $\sigma_{trans}(y)$ depends on the transverse diffusion along the drift path. It can be parametrized as [5] $\sigma_{trans}(y) = \sqrt{\sigma_0^2 + \frac{D_t^2 \times y}{n_{cl}^{el}}}$, where

- σ_0 = best achievable resolution for zero drift distance

- $D_t =$ constant of transverse diffusion
- $n_{cl}^{el} =$ number of primary electrons contributing to a cluster.

Using the information from the Si-stripe telescope the events were sorted into slices of 0.5 mm along y . The spatial resolution $\sigma_{mean}(y)$ was determined for each bin. The best resolution at zero drift was extrapolated from a fit of $\sigma_{trans}(y)$ to the measured values $\sigma_{mean}(y)$ in Fig.4. Including systematic errors the result for the standard GEMs was $\sigma_0 = 22 \pm 2 \mu\text{m}$ and for the small pitched GEMs $\sigma_0 = 15 \pm 1 \mu\text{m}$. This suggests that the GEM hole pitch of $\geq 50 \mu\text{m}$ might matter.

2.4 Effect of GEM pitch

In view of the small values of spatial resolution at drift distances close to the first GEM ($\approx 20 \mu\text{m}$) possible effects of discrete nature as the pitch of the GEM holes and even the finite pitch of the readout has to be considered. In order to investigate this effect in the present setup, a spatial Fast Fourier Transformation (FFT) on the distribution of the centroids from the track fit is performed. For this all y -centroids of tracks, passing near the first GEM, are projected onto the chip's x -axis, which is approximately orthogonal to the tracks. The distribution is shown in Fig. 5a, already here a periodic structure is seen. This observation matches the result of the FFT transformation on this data where a signal of $(8.39 \pm 0.04) \text{ mm}^{-1}$ spatial frequency is apparent, which corresponds to a period of $(119.2 \pm 0.6) \mu\text{m}$, shown in Fig. 5b. This is in very good agreement with the projected GEM-hole pitch of $120 \mu\text{m}$ in this direction. Since the GEM is slightly rotated against the coordinate system of the chip, the maximum of the spatial frequency amplitude

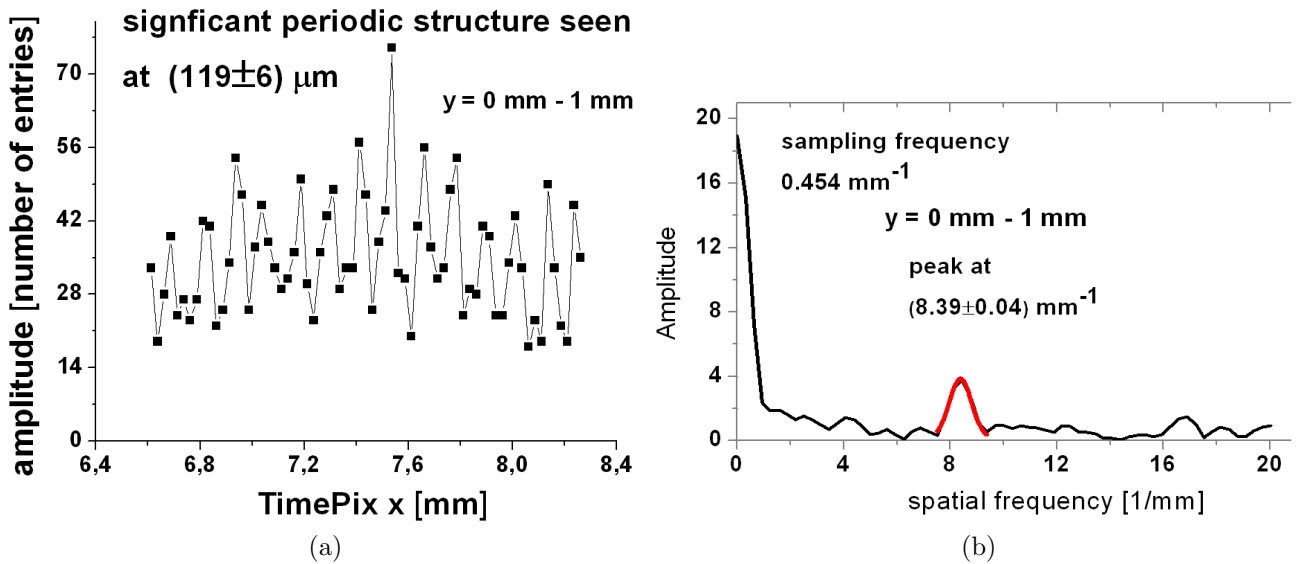


Figure 5: a) Projected distribution of x -coordinate of calculated cluster centres along the track axis.
 b) Fast Fourier Transformation of the distribution in a).

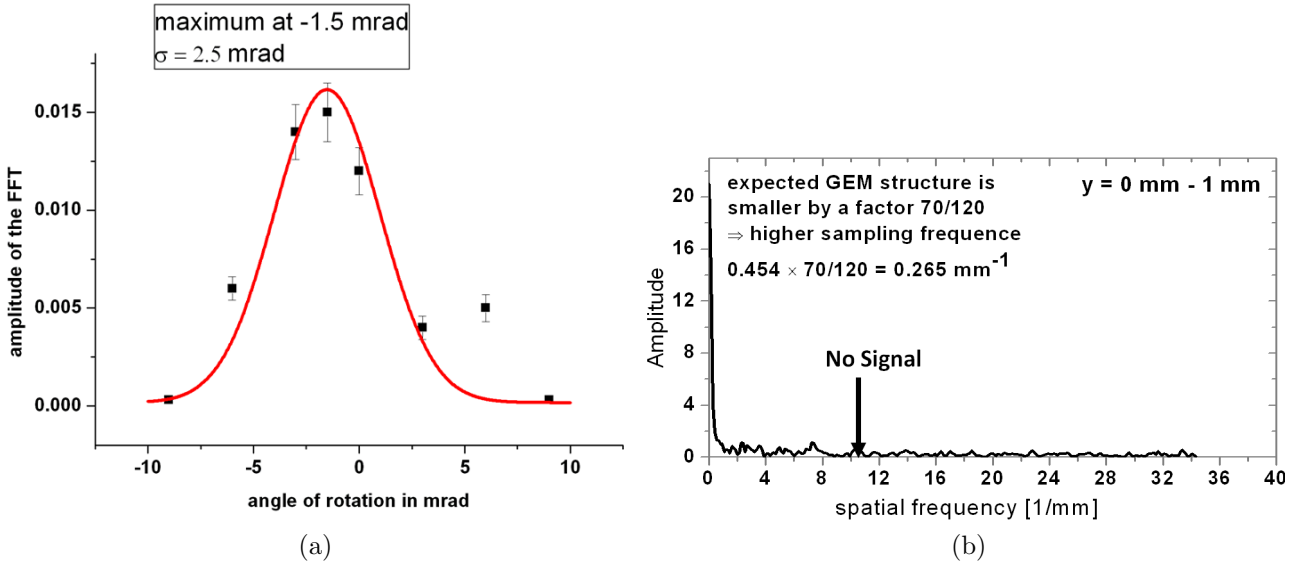


Figure 6: a) Amplitude of the peak in the FFT as function of the rotation angle of the GEM.
 b) Fast Fourier Transformation of the projected distribution of x -coordinate from calculated cluster centres along the track axis, after rotation of the GEM by 90° .

occurs at an angle of 0.11° . As seen in Figure 6a the FFT-signal disappears within a small angular range of $\pm 0.4^\circ$. It is also interesting to note that the signal disappears for large drift distances beyond 1.0 mm. Here the averaging due to the transverse diffusion of primary electrons of multi-electron clusters starts to dominate.

A rotation of the GEM by 90° results in a projected pitch along the tracks of $70 \mu\text{m}$, see Fig. 6b. In this case a rotation-scan as described above did not reveal any signal that would be expected at a period of $70 \mu\text{m}$. One should also note that the effect of a possible discreteness of the centroids affects the deviation from a fitted line only if the track is nearly parallel to the GEM-hole-pattern. Then σ_0 would naively be $120 \mu\text{m}/2=60 \mu\text{m}$, if the electrons passed strictly parallel and in between two rows of holes. The existing angular dispersion of about 1° for the tracks is expected to greatly suppress possible systematic effects.

2.5 Time Walk Correction

The TIME-measurements showed a dependency on the pulse height (“time walk”) as displayed in Fig. 7a. TIME-values measured next to pixels with small TOT seemed to arrive systematically later compared to TIME-values which lay close to pixels with a large TOT-value. From the TOT-TIME-correlation a correction function had been derived and was applied to the mixed mode data. Fig. 7b shows the deviations of

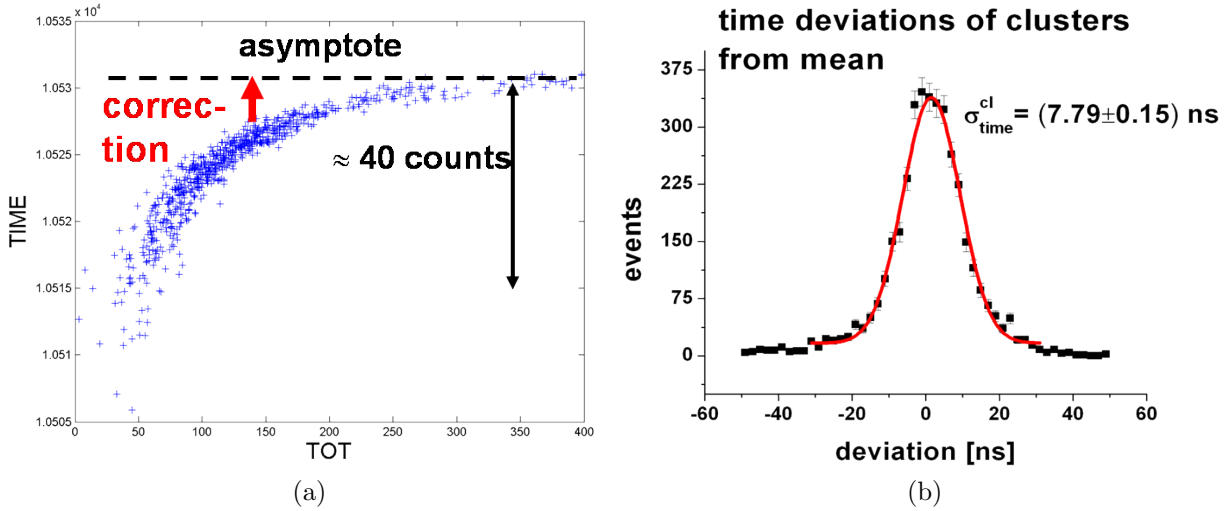


Figure 7: a) Correlation of TOT vs. TIME. Signals in the vicinity of pixels having small TOT-counts seem to arrive systematically later than signals next to pixels with a high TOT-counts (“time walk”).
 b) Plotted are the deviations of corrected TIME values from the corrected mean time in the corresponding event. A fit to these values results in a σ_{time} of ≈ 8 ns.

(corrected) TIME-values at the center of a cluster relative to the mean¹ of the corresponding event. The time resolution was as good as 8 ns, which is smaller than the clock period.

3 Further R&D activities

3.1 Post Processing

Post processing is aimed to increase the pixel size for optimizing the readout granularity. As shown in Fig. 8a the first step was to have three out of four neighboring pixels passivated, while the fourth pixel had been left open. This increased the pixel size to $110 \mu\text{m} \times 110 \mu\text{m}$. As shown in Fig. 8b first tests with a MediPix2 chip are promising. Possible reasons for the crosstalk observed between adjacent pixels have also been under investigation.

3.2 Development of an UV-Laser Test-Bench for Characterisation of MPGDs

Currently an UV-laser test bench is being set up. As indicated in Fig. 9 the laser will release (single) photo electrons from the drift cathode. After a short drift the photo

¹This was determined per event by averaging over all TIME values at the cluster centroids.

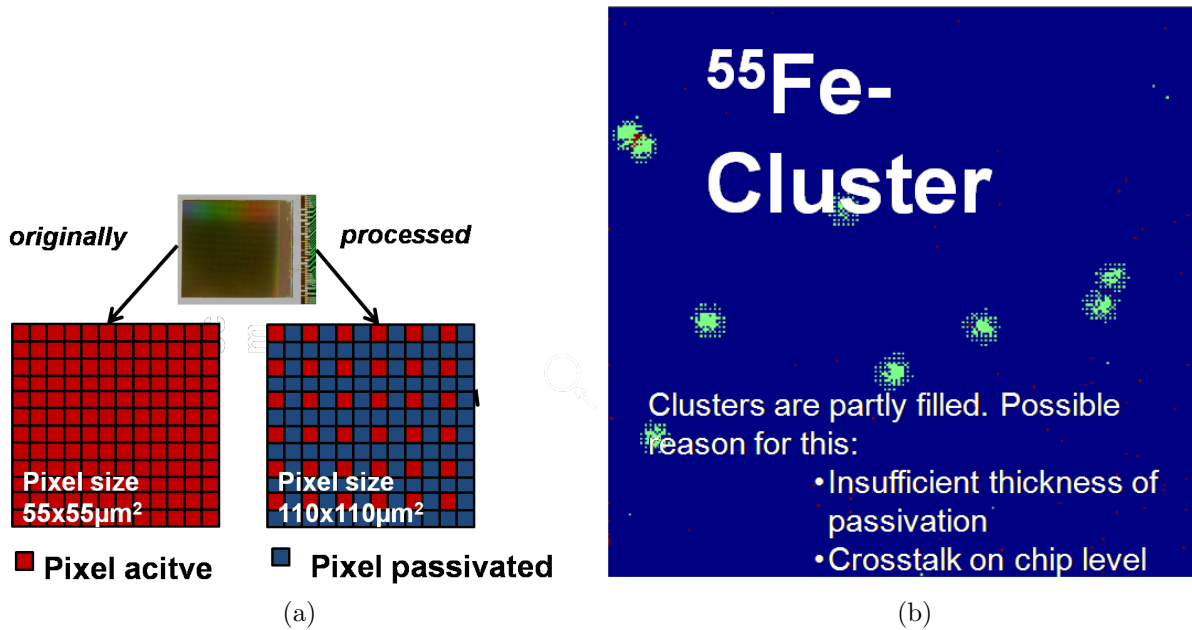


Figure 8: a) Illustration of the post processing to enlarge the effective pixel size. Out of four neighboring pixels three are passivated (blue), while one is left open (red).
 b) Event taken with ^{55}Fe source.

electrons are amplified and recorded by the device under test. The correlation in space and time of the charge signal will allow to study detection efficiencies and amplification processes for various combination of MPGDs plus pixel readout.

3.3 Software development for Integration in the EUDET test beam

At DESY the Eudet telescope and the Large Prototype are being finalized. For successful test beam runs a software has to be developed to integrate the existing TimePix DAQ

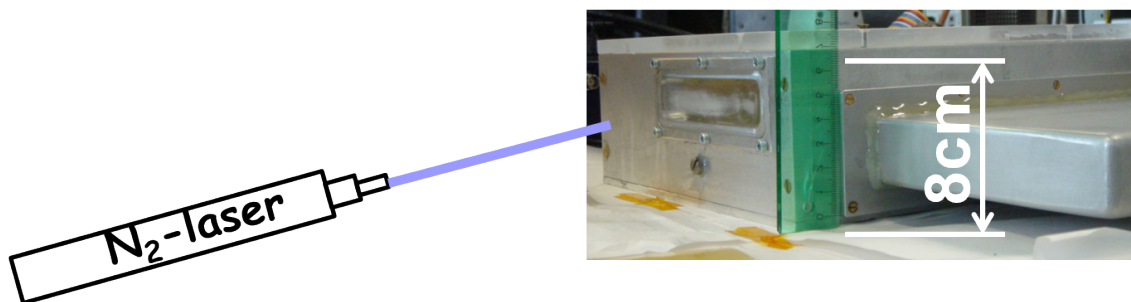


Figure 9: An UV-Laser will be directed onto the drift cathode. There it will release photo electrons which, after a short drift, will be amplified by the device under test.

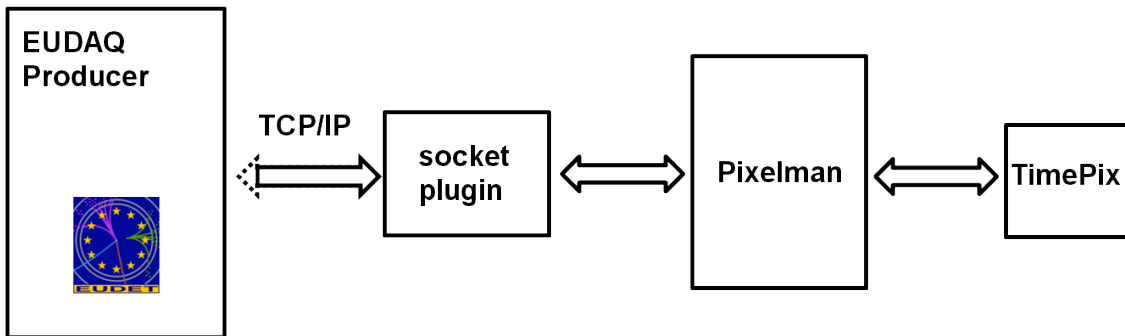


Figure 10: Illustration of the planned communication between the EUDAQ framework and the TimePix DAQ (Pixelman).

into the Linux based framework there. This is especially challenging as the TimePix software is Windows based and the source coded is not available under an open-source-license. Therefore EUDET-participants from DPNC Geneva, University of Bonn and Freiburg are working on a so called "Producer", which uses the socket interface allowing an inter-platform communication. As depicted in Fig. 10 standard network protocols such as TCP/IP will be used for data communication between EUDAQ and a Producer-Plug-In for the TimePix DAQ.

4 Conclusion

It was shown that the point resolution for short drift distances is better than $20\ \mu\text{m}$. The achieved time resolution is better than $10\ \text{ns}$ at $100\ \text{MHz}$ clock frequency. With the results from this small test setup first steps towards a new generation of gaseous detectors were taken. The investigations will be continued with prototypes such as the Large Prototype of the LCTPC and within the RD51 collaboration. Combining the advantages of MPGDs with the high readout granularity, developed in the field of semi-conductor detectors, opens up a completely new and wide range of applications not only high energy physics, but also in other fields of detector instrumentation.

Acknowledgement

We thank the Freiburg Material Research Center for their assistance and for performing the post processing.

This work is supported by the Commission of the European Communities under the 6th framework program "Structuring the European Research Area", contract number RII3-026126.

References

- [1] X. Llopart Cudie, “Design And Characterization Of 64-K Pixels Chips Working In Single Photon Processing Mode”, CERN-THESIS-2007-062;
- [2] M. Milite, “The internal structure of charmed jets in photoproduction at HERA and tests of the ZEUS microvertex silicon sensors,” , DESY-THESIS-2001-050;
- [3] http://www.nikhef.nl/pub/experiments/medipix/files/muros2.0_manual.pdf
- [4] A. Bamberger, K. Desch, U. Renz, M. Titov, N. Vlasov, P. Wienemann and A. Zwerger, “Readout of GEM detectors using the Medipix2 CMOS pixel chip,” Nucl. Instrum. Meth. A **573** (2007) 361 [arXiv:physics/0611229].
- [5] C. Amsler *et al.* [Particle Data Group], “Review of particle physics,” Phys. Lett. B **667** (2008) 1.